SEED METERING DEVICE MOTOR-DRIVEN SYSTEM BASED ON CANOPEN PROTOCOL

Xinhui SUI[1], Kexin XU[2], Jianqiao WANG[3], Tianhao JING[4], Yulong CHEN[5*], Meng ZHANG[6]

Conventional motor driving system for seed metering device mostly uses the brushless DC motor. However, the brushless DC motor needs to be connected to an external driver and encoder. It's difficult to control multiple motors. For this problem, the study designed a motor driving system based on CANopen protocol. The system used an integrated motor to replace brushless DC motor. The motor control strategy adopted the incremental PID algorithm. Detection test of seeding performance index showed, when the operation speed of the machine was 2-6 km·h^{-1}, the qualified seeding rate was higher than 95.6%, the reseeding rate was lower than 2.39%, the missing seeding rate was lower than 2.01%, and the coefficient of variation was less than 7.63%. When the forward speed was 8-12 km·h^{-1}, the qualified rate was higher than 91.63%, the reseeding rate was lower than 3.98%, the missing seeding rate was lower than 4.39%, and coefficient of variation was less than 12.01%.

Keywords: Integrated motor, CANopen, PID, Cooperative control

1. Introduction

Conventional seed metering devices were driven by ground wheels. This method is limited by soil condition and forward stability. With the development of intelligent control technology in agricultural seeding, the motor driving system for seed metering device emerged. The motor driver avoids the influence of external factors effectively. Zhai et al. designed a motor driving system that reduces uneven seeding caused by ground wheel slippage [1]. Du et al. developed a control system based on the FOC algorithm [2], which had better speed control performance,

[1] College of Agricultural Engineering and Food Science, Shandong University of Technology, Zibo, 255000, China, e-mail: 19862513127@163.com
[2] College of Agricultural Engineering and Food Science, Shandong University of Technology, Zibo, 255000, China, e-mail: 2536570601@qq.com
[3] College of Agricultural Engineering and Food Science, Shandong University of Technology, Zibo, 255000, China, e-mail: 19811709920@163.com
[4] College of Agricultural Engineering and Food Science, Shandong University of Technology, Zibo, 255000, China, e-mail: 18353169398@163.com
[5] Modern Agricultural Equipment Research Institute, Shandong University of Technology, Zibo, 255000, China, e-mail: cyl06471@sdut.edu.cn
[6] Weichai Lovol Intelligent Agricultural Technology Co., Ltd, Weifang, 261206, China, e-mail: 411225919@qq.com

torque stability and superior seeding quality. Yao et al. designed a DC motor driving system for seed metering device and found that the fuzzy PID algorithm was better than the conventional PID [3]. Ding et al. designed a rotational speed compensation system to ensure the uniformity of seeding spacing in each row [4]. Wang et al. designed a motor driving system based on genetic algorithm fuzzy PID and found that its performance was better than the conventional fuzzy PID [5]. These studies shows that motor driving has excellent seeding performance. However, conventional control systems use brushless DC motors [6], which need an external driver and encoder. It is difficult to achieve the control of multi-rows seeding and long-distance operation.

For these problems, this system selected a CAN communication control strategy based on CANopen protocol. This system adopted an integrated motor with a built-in driver and absolute encoder which supported remote control. A communication protocol conforming to the ISO11783 standard was designed to achieve the control of three motors, which ensured the system achieved the control of multi-row seed metering devices and had better accuracy and stability.

2. Materials and Methods

2.1 Motor-driven system components and workflow

The motor driving system was composed of a host controller, a seeding unit controller, an IPC, an ATK-NEO-6M GPS module plus an external antenna, and an STM4248B-CANopen-MA-OFS integrated stepper servo motor [7]. The overall workflow of the control system is shown in Fig.1. When the seeding system started to work, the GPS module with the cooperation of the external antenna measured the forward speed of the machine, and transmitted data to the STM32 microcontroller through serial communication [8], then the target speed of the motor was obtained in the microcontroller and the corresponding SDO message instruction was issued to the motor. Absolute encoder inside the motor measured actual rotational speed. Finally, the incremental PID algorithm was used to achieve the closed-loop control of the motor speed based on the difference between the target rotational speed and actual rotational speed, which ensured the actual rotational speed was close to the target speed [9].

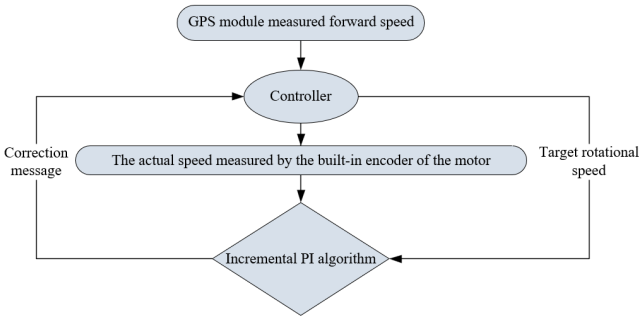

Fig. 1. Overall workflow diagram of the control system

2.2 Hardware design of motor driving system

The motor driving system used STM32F103VET6 microcontroller as host controller. The microcontroller schematic is shown in Fig. 2, consisting of CAN communication conversion circuit, 5V-3.3V step - down circuit, USB-USART conversion circuit, crystal oscillator circuit, reset circuit, BOOT circuit, GPS sensor circuit [10]. The main controller chip had dual bxCAN interfaces, which supported CAN2.0A and CAN2.0B, and met requirements of ISO 11898. Through the CAN transceiver, it could achieve communication between the host controller and integrated stepping servo motor [11].

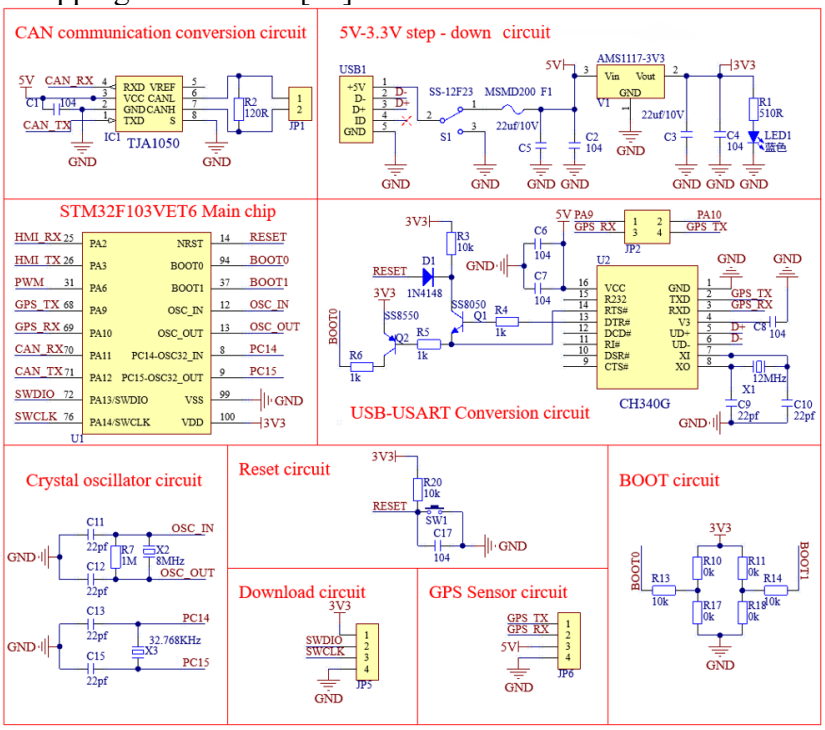

Fig. 2. STM32 microcontroller system schematic diagram

2.3 Software design of motor driving system

2.3.1 Motor selection

A seed metering device torque measurement test bench measured the required torque and rotational speed to determine the type of motor. Brushless DC motors have the characteristics of low cost and easy of control, so they are used as the test motor for torque measurement test bench. The test bench consisted of a computer, RS485 communication module, 24 VDC power supply, brushless DC geared motor, coupling, dynamic torque sensors, air-suction seed metering device, motor driver, negative pressure fan, and so on.

Since the drive mode of the air-suction seed metering device is divided into center shaft driving and circumferential driving [12], it is necessary to use these two driving modes for torque measurement test respectively. In the central shaft driving torque measurement test, a brushless DC geared motor, coupling, dynamic torque sensor and seed metering disc center shaft were coaxially connected, to measure the torque at different speeds. For circumferential driving torque measurement, a brushless DC geared motor shaft, coupling, dynamic torque and a drive component were coaxially connected. The driving component had a gear whose tooth number was 16 and module was 1.6 to drive the seed metering disc, which measures the rotational speed in different speeds. The physical connections in both driving modes are shown in Fig. 3.

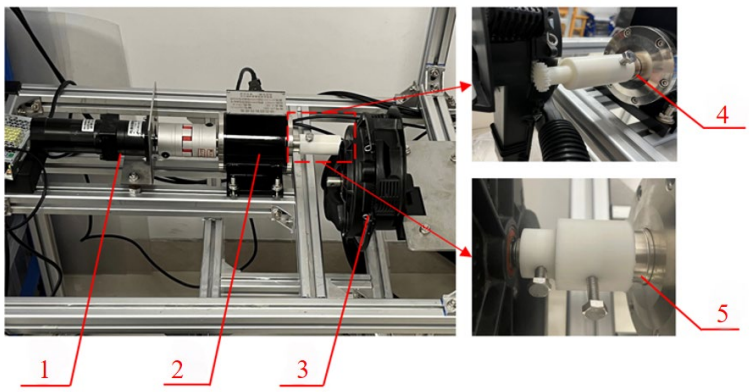

Fig. 3. Seed metering device torque measurement test bench. 1. Brushless DC geared motor, 2. Dynamic torque sensors, 3. Air-suction seed metering device, 4. Circular driving mode, 5. Center driving mode.

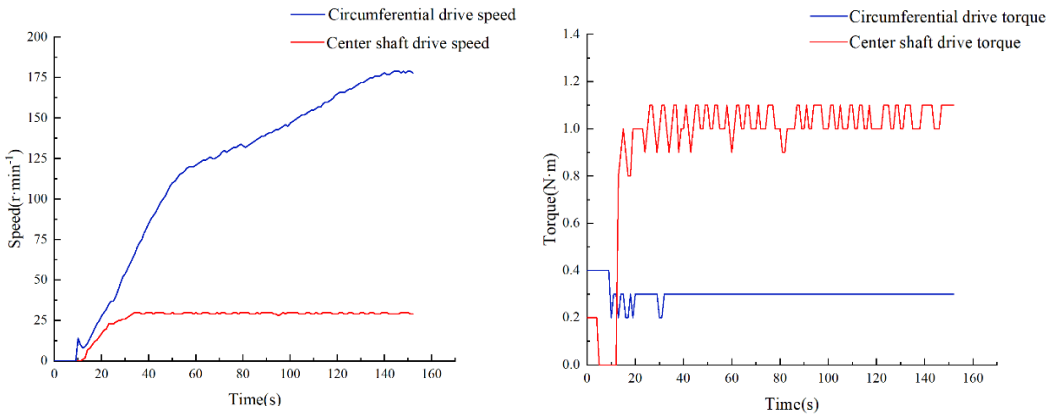

(a) (b)

Fig. 4. Center shaft vs. circumferential driving

The torque and rotational speed information obtained in real time by the torque measurement software through RS485 communication is shown in Fig. 4 (a) and Fig. 4 (b).

Analysis of Fig. 4 (a), in the center shaft driving mode, the motor speed increases from 0 to 30 r·min^{-1} between 10 and 35 s and then remains steady. In the circumferential driving mode, the motor speed increases from 0 to 180 r·min^{-1} between 0 and 140 s, reaches a peak value.

Analysis of Fig. 4 (b), in the center shaft driving mode, the interval between 0 and 13 s is the process of defining the zero value for the torque. Subsequently, there is a rapid increase from 0 to 1 N·m between 13 and 20 s, and then it remains relatively stable. In circumferential driving mode, the torque starts with a maximum value of 0.4, then decreases to 0.3 and keeps stable.

The analysis shows that the torque required for the circumferential driving is lower, so the circumferential drive method is selected to drive the seed metering device.

As can be seen from Fig. 4 (b), the maximum torque for driving the seed metering device is 0.4 N·m, so the output torque of driving motors should be greater than 0.4 N·m within a certain rotational speed range.

The theoretical rotational speed of the driving motor for seed metering disc can be calculated from the forward speed:

$$N_{mt}=\frac{60Vi}{SZ} \tag{1}$$

Where N_{mt} is the theoretical rotational speed of the driving motor, r·min^{-1}, V is the forward speed of the seeder, m·s^{-1}, i is the deceleration ratio, S is the number of suction pores on the seed metering disc, Z is the target seed spacing, m.

The target seed spacing is 25 cm, the number of suction pores on the seed metering disc is 27, maximum forward speed is 12 km·h^{-1}, parameters of the circumferential driving gear are 1.6 modulus and 16 teeth and circumferential gear for the seed metering disc are 1.6 modulus and 106 teeth, the deceleration ratio is 6.625:1, and maximum target rotational speed of driving motor is 196.30 r·min^{-1}. So maximum rotational speed of motor should be greater than 196.30 r·min^{-1}, rotational speed should be greater than 196.30 r·min^{-1}.

During the seeding process, the seeding device drive motor must reach the target speed as quickly as possible. At the same time, due to operational requirements, the motor will frequently undergo operations such as start - up, shut - down, and speed regulation. Stepper motors, compared with DC motors, require less time to reach the target speed because of their unique working characteristics, and their working state remains very stable throughout the entire operation process. The driving motor is a STM4248B-CANopen-MA-OFS integrated stepping servo motor, its maximum output torque of motor is 0.5 N·m and maximum rotational speed is 600 r·min^{-1}, it uses CANopen protocol, CiA402 communication sub-protocol and built-in absolute encoder. The physical appearance and parameters of the motor are shown in Figure 5.

the physical object of the motor	Motor parameters	Parameter values
	Maximum torque（N·m）	0.5
	Maximum rotational speed（r·min^{-1}）	600
	Input voltage（V）	10-30
	rated current（A）	1.68
	Step angle（° ）	1.8
	Communication protocol	CANopen
	Communication sub protocol	CiA402
	Number of phases	2
	Motor weight（kg）	0.41
	Motor body dimensions（mm）	66.5*42*42
	Encoder type	Incremental encoder
	Operating mode	Position mode, speed mode , etc

The physical appearance and parameters of the motor.

The installation of the seed metering device is shown in Fig. 6.

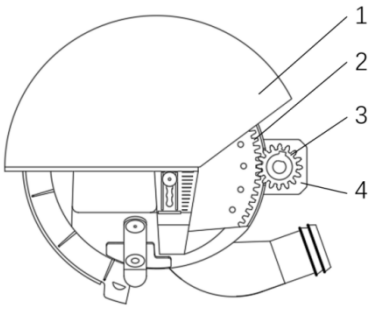

Fig. 6. The installation of seed metering device. 1. Air-suction seed metering device, 2. Seed metering disc Circumferential gear, 3. Driving gear of motor, 4. Integrated stepper servo motor.

2.2.2 Motor Control Strategy

STM4248B-CANopen-MA-OFS integrated stepper servo motor used CAN bus protocol based on ISO11898 to communicate, while used application layer specification based on CANopen protocol to define communication rules and data exchange [13]. The CiA402 device sub-protocol redefined the meaning of the data inside the motor based on the CANopen protocol. The communication between the controller and the motor was mainly transmitted through PDO and SDO messages. This system achieved the control of the motors through sending and receiving SDO messages [14].

This system was intended to control three integrated motors at the same time. Three motors were connected in parallel with each other as a slave, through the three outputs of CAN CAN_H, CAN_L, GND to communicate with the master, both ends need to be connected to the 120 Ω termination resistors. Since the master controller STM32F103VET6 microcontroller itself came with a resistor, it was only necessary to connect a terminal resistor between CAN_H and CAN_L of the third motor at the outermost end to achieve the synchronous control, as shown in Fig. 7.

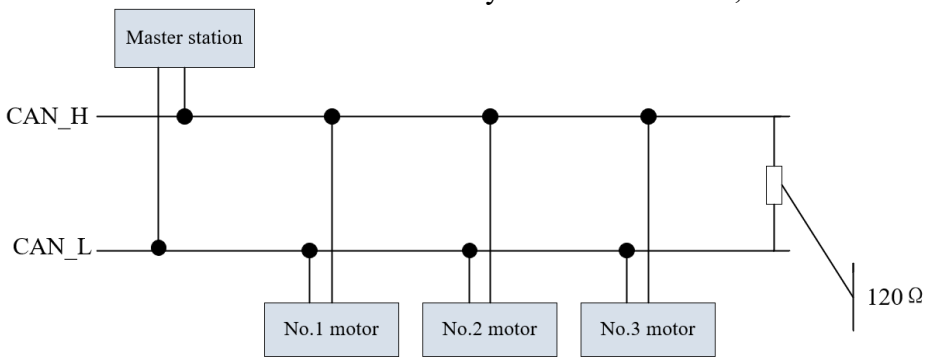

Fig. 7. CAN communication connection diagram for integrated servo motor

The implementation of the CANopen protocol included initialization module, message-sending module, message-receiving module, network node management module, etc. Therefore, the master station STM32 could achieve the control of motors by initializing, reading and writing the specific object dictionary inside the motor through the CAN bottom communication algorithm The specific implementation process was as follows: first set the NMT network management operation status for network initialization and check the device status, then set the resolution and set the CiA402 state machine to control the drive, the working mode was set to the contour speed mode to complete the initialization of the motor. Finally, controlled the motor operation status by sending a specific data format message, and receiving information in real-time to obtain the motor's speed. The flow of operation for controlling the motor is shown in Fig. 8.

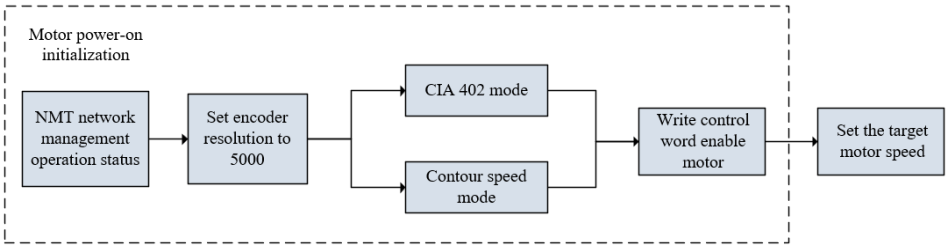

Fig. 8. Integrated stepper servo motor control flowchart

The motor encoder resolution is set to 5000, get the formula 2. Based on formula 1 and 2, got formula 3 for writing the value of the motor speed in CAN communication.

$$N_{mt}=\frac{3\times Speed}{250} \tag{2}$$

$$Speed=\frac{5000Vi}{SZ} \tag{3}$$

Where N_{mt} is the theoretical rotational speed of motor, $r\cdot min^{-1}$, V is the forward speed of machine, $m\cdot s^{-1}$, i is the deceleration ratio, *Speed* is the value to write rotational speed of motor in CAN communication.

2.2.3 Motor control algorithm

This system used the incremental PID algorithm, which could be considered to consist of *first-order differential term*, *proportional term* and *second-order differential term*. Compared to the others, the incremental PID algorithm did not need to accumulate the error between target and actual values, which was less computationally intensive and saved processor storage space. Each control output was relative to the last change in the value, the error rate was low, the closed-loop algorithm system operation was more stable. In the latter part of the closed-loop

motor speed control test found that the incremental PID algorithm control of the *second-order differential term* on the system had little effect. Therefore, the incremental PI algorithm was chosen to achieve the closed-loop control of motor speed Its motor speed incremental PI algorithm control schematic diagram is shown in Fig. 9.

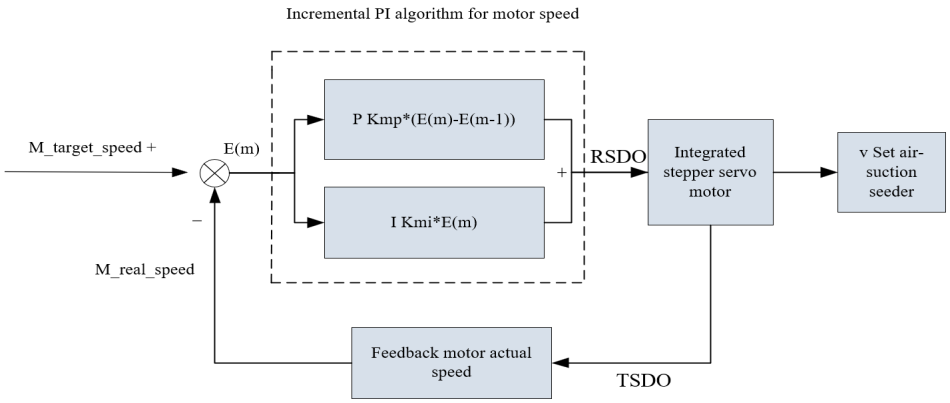

Fig.9. Motor speed incremental PI algorithm control schematic diagram

Where *M_target_speed* is the motor's target speed, *M_real_speed* is the motor's actual speed.

The motor speed incremental PI algorithm equation is:

$$\Delta V_m = K_{mp}\big(E(m)\text{-}E(m\text{-}1)\big) + K_{mi}E(m) \tag{4}$$

Where ΔV_m is the dynamic change of the motor speed incremental PI control output in two adjacent moments, $E(m)$ is the difference between the target speed and the actual speed of the motor in m moment, $E(m\text{-}1)$ is the difference between the target speed and the actual speed of the motor in $m\text{-}1$ moment, K_{mp} is the coefficient of *proportional term* in closed-loop motor speed control system, K_{mi} is the coefficient of the *integral term* in closed-loop motor speed control system.

The principle of the incremental PI algorithm is as follows: First, set the target speed of the motor. Then, the internal encoder of the motor obtains the actual speed signal of the motor. Based on the difference between the target speed and the actual speed, the incremental PI algorithm will reduce the error according to certain proportional and integral coefficients, enabling the actual speed to gradually approach the target speed and thus completing the speed control of the motor.

2.3 Experimental design

In order to verify the feasibility of the selected motor and control algorithm, an experimental - scale test was carried out to evaluate the seeding performance. Golden Sunshine No. 6 corn seeds were selected in the experiment, with a thousand - kernel weight of 333 g and a bulk density of 744 g/L. The shape was like a semi-

horseshoe. The seeding device adopts an air-suction seed metering device, and the diameter of the suction holes on the seed metering disc is 4.5 mm, the number of suction holes is 27. It is equipped with a seeding guide tube. Brushless DC negative - pressure fans are selected for the suction fan, which are paired with a fan driver. The driving motor is controlled by an STM32 single - chip microcomputer, and the computer is responsible for inputting instructions to the single - chip microcomputer. Three sets of seeding devices are installed to verify the multi - row coordinated control ability of the motor. The bench - scale test is carried out on the JPS - 12 seeder performance testing platform, as shown in Figure 11.and the relevant tests were mainly conducted on the performance test bench of the JPS-12 seed platter. The test bench is shown in Fig. 10.

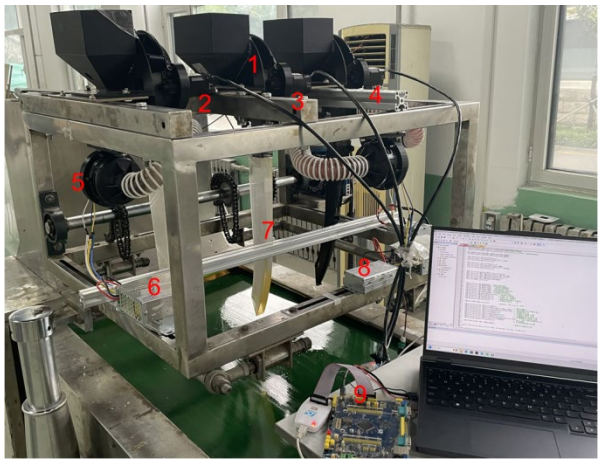

Fig. 10. Motor driving seeding speed control system. 1. Air suction seed metering device, 2. No.1 motor, 3. No.2 motor, 4. No.1 motor, 5. Negative pressure fan, 6. AC 220 V-DC 12 V Power Module, 7. Seed tube, 8. Negative pressure fan driver, 9. Controller.

To verify the feasibility of the incremental PID in this speed control system and performance of the motor driving system, the motor constant speed closed-loop control test, the motor speed dynamic response test, and the seeding performance index detection test were conducted. PID could make the actual speed closely match the operating curve of the target speed, enable the actual speed to respond to changes of target speed in real-time quickly and test the seeding performance of the motor driving control system.

2.3.1 Motor fixed speed closed-loop control test

The driving motor operated in profile speed mode in CiA402 mode. The acceleration-deceleration curve type was linear, which had advantages of quick response and smooth operation. However, during the seeding process, the seed metering disc would inevitably be affected by its mechanical mechanism, seeds,

etc. The system used a STM32 microcontroller and an incremental PI algorithm to achieve closed-loop control of the seeding shaft speed.

Formula 2 explained, when the forward speed is 2-12 km·h^{-1}, the target speed of the seeding shaft driving motor was obtained. After comparing results, a trial-and-error method was used to determine the parameters of the motor's incremental PI closed-loop control when the forward speed was 2 km·h^{-1}, including the K_{mp} equaled 450 and K_{mi} equaled 2.25. Based on these parameters, to determine the response of the motor speed at other speeds.

2.3.2 Motor speed dynamic response test

To explore the response performance of the motor speed when the machine's forward speed changed, a laboratory simulation experiment was conducted on the following performance of the driving motor and machine. By sending different forward speeds, the machine's forward speed was between 2 and 12 km·h^{-1}. Stepwise acceleration and deceleration changes were performed at intervals of 2 km·h^{-1}.

2.3.3 Seeding performance index assessment test

To explore the impact of different forward speeds on the performance of the seed metering device, conducted a seeding performance assessment test. The seed spacing was set to 25 cm, and the machine tool operation was simulated under different speed conditions of 2, 4, 6, 8, 10, and 12 km·h^{-1}. The performance test bench of the JPS-12 seed platter was used to test the three rows of seed metering devices at a single time. Continuously collected 251 seeds, repeated the test three times, and obtained the seed spacing information in real-time. The seed spacing qualified seeding index A (%), reseeding index D (%), missed seeding index M (%) and coefficient of variation C (%) of the three-row seed metering device under the condition of fixed spacing were calculated, and were used as the evaluation standard for seeding performance.

3. Test results

3.1 Closed-loop control test of the motor with fixed speed

Origin software was used to process the data to obtain the motor speed response curve at different forward speeds, shown in Fig. 10. The closed-loop control effect was judged by the response time, adjustment time, steady-state error, and overshoot in the response curve.

The response curve can be seen in Fig. 10. The response results of the motor at the set target speed are shown in Table 1.

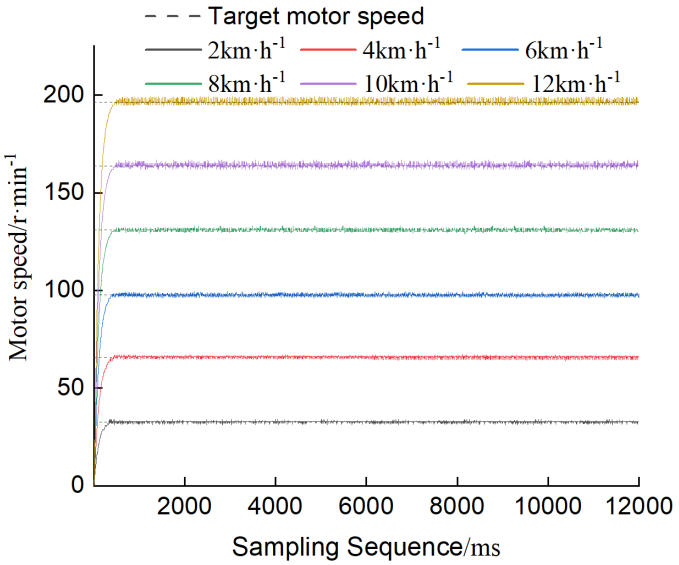

Fig. 10. Motor speed response curve at different forward speeds

Table 1

Response parameters of motor speed at different forward speeds

Target speed (r·min^{-1})	Response time (ms)	Adjustment time (ms)	Steady-state error(r·min^{-1})	Overshoot (%)
32.72	375	416	1.28	2.61
65.46	439	475	1.54	2.35
98.11	464	498	1.92	1.93
130.84	496	536	2.16	1.65
163.57	511	557	2.43	1.48
196.29	549	603	2.71	1.38

It can be seen from the data in Table 1 that when the motor target speed is 32.72-196.29 r·min^{-1}, the average response time is 472.33 ms, the difference is 55.66 ms, the average adjustment time is 514.17 ms, the difference is 60.05 ms, the motor features a rapid speed response, with both short response and adjustment times, and operates under a light load. When the motor target speed are 32.72-65.46 r·min^{-1}, 98.11-130.84 r min^{-1}, and 163.57-196.29 r min^{-1}, the average steady-state errors are 1.41 r min^{-1}, 2.04 r min^{-1} and 2.57 r min^{-1}, respectively, and the difference is 0.47 r·min^{-1}.The average overshoot is 2.48%, 1.79%, and 1.43%, respectively, and the difference is 0.44%. The steady-state error and overshoot of the system have little difference in different target speed ranges of the motor. Therefore, when K_p equals 450 and K_i equals 2.25, the metering shaft driving motor has high closed-loop control accuracy at different target speeds.

3.2 Motor speed dynamic response test

Vofa+ software outputted the dynamic response data of the actual speed of the motor at different forward speeds. The rotational speed response data is shown in Table 2.

Table 2

Motor actual speed dynamic response results

Type	Speed(km·h^{-1})	Motor target speed (r·min^{-1})	Rising time (ms)	Adjustment time (ms)	Steady-state error (r·min^{-1})	Overshoot (%)
Accelerate	0->2	32.37	375	416	1.04	3.39
	2->4	65.46	432	475	1.63	2.49
	4->6	98.12	464	498	1.89	0.69
	6->8	130.84	496	536	2.32	0.88
	8->10	163.57	511	557	3.57	1.30
	10->12	196.30	543	603	4.08	1.88
Decelerate	12->10	163.57	502	540	3.23	1.19
	10->8	130.84	453	496	2.05	0.75
	8->6	98.12	417	465	1.72	0.62
	6->4	65.46	386	424	1.36	2.35
	4->2	32.37	338	395	0.87	2.37
	2->0	0	145	0	0	0

It can be seen from Table 2 that when the speed gradually increases with an interval of 2 km·h^{-1}, the average rise time, adjustment time, steady-state error and overshoot of the seeding plate driving motor speed are 470.17 ms, 514.17 ms, 2.42 r·min^{-1}, 1.77% ,the difference are 55.06 ms, 60.05 ms, 1.07 r·min^{-1}, 0.94%, respectively. When the speed decreases successively at intervals of 2 km·h^{-1}, the driving average rise time, adjustment time, steady-state error and overshoot of the motor speed are 373.5 ms, 386.67 ms, 1.54 r·min^{-1}, 1.21%, and the differences are 114.28 ms, 179.15 ms, 1.06 r·min^{-1}, 0.88%, respectively. Compared with the decreasing and increasing forward speed, the average rising time and adjustment time of the seeding plate driving motor speed are shortened by 96.67 ms and 127.5 ms, the average steady-state error and overshoot are 0.88 r·min^{-1} and 0.56%. Results are mainly due to the motor itself in deceleration start-up change rate is greater than in acceleration start-up change rate caused.The average rising time and adjustment time of the driving motor speed are 421.84 ms and 450.42 ms. The average steady-state error and overshoot are 1.98 r·min^{-1} and 1.49%. Therefore, the system has features of fast response and high stability.

3.3 Seeding performance assessment test

Results of the seeding performance assessment test are shown in Table 3. As the forward speed increases, the seeding performance generally shows a

trend. The qualified seeding rate of the three-row metering device does not change much when the forward speed is 2-6 km·h^{-1} and remains above 96.14%. The reseeding rate is lower than 2.26%, the missing seeding rate is lower than 1.6%, and the variation coefficient is less than 6.87%. When the operating speed reaches 8-12 km·h^{-1}, the qualified seeding rate drops significantly to 92.03%, the reseeding rate is lower than 3.72%, the missing seeding rate is lower than 4.25%, and the variation coefficient is less than 11.55%.

The results met the requirements for precision seeding by bench testing with reference to International Standard ISO 7256/1.

Table 3

Seeding performance indicators at different forward speeds

Speed (km·h^{-1})	*A* (%)	*D* (%)	*M* (%)	*C* (%)
2	97.61	1.59	0.8	6.32
4	96.14	2.26	1.6	6.87
6	97.21	1.46	1.33	6.8
8	95.88	1.99	2.13	7.77
10	92.83	3.05	4.12	9.88
12	92.03	3.72	4.25	11.55

4. Conclusion

(1) Taking the air-suction seed metering device as the research object, the seed metering disc has a 1.6-mold 16-tooth gear. A seed metering device torque measurement test bench was built. Through the torque measurement test of the central axis drive and the circumferential drive seed metering device, the circumferential drive and metering device were selected. The measured torque required for the circular drive is no more than 0.4 N·m, and an integrated stepper servo motor based on the CANopen protocol is selected as the seeding drive motor.

(2) The closed-loop control test of motor speed based on the incremental PI algorithm, where K_{mp} and K_{mi} are 450 and 2.25, and the operating speed is 2-12 km·h^{-1}. In the fixed speed and variable speed tests, the average adjustment time, steady-state error, and overshoots are 514.17 ms,2 r·min^{-1}, 1.9%, 450.42 ms, 1.98 r·min^{-1}, and 1.49%, respectively. The seeding drive motor has high control accuracy at different target speeds, rapid dynamic response, and high system stability. Meanwhile, it indicates that the control algorithm of the motor exhibits excellent performance in terms of low computational load and space - memory savings.

(3) The seeding performance assessment test shows that the higher the forward speed of the machine, the lower the seeding quality. In the low-speed range of 2-6 km·h^{-1}, the qualified seeding rate of the three seed metering devices is higher than 95.6%, the re-seeding rate is lower than 2.39%, and the missing seeding rate is lower than 2.01%, the variation coefficient is less than 7.63%, the qualified seeding rate of the three metering devices in the high-speed range of 8-12 km·h^{-1} is

higher than 91.63%, and the re-seeding rate is lower than 3.98%, the missing seeding rate is less than 4.39%, and the coefficient of variation is less than 12.01%.

This system can achieve precision seeding of corn and complete coordinated control of multi-row seed metering devices based on accurate speed control. This system can provide a reference for the technology of motor driving control system for multi-row seed metering device.

REFERENCES

[1] *JB. Zhai, JF. Xia, Y. Zhou, S. Zhang*. "Design and experimental study of the control system for precision seed - metering device", International Journal of Agricultural and Biological Engineering, **vol. 7**, no.3, 2014, pp.13 – 18.

[2] *ZH, Du. L, Yang. DX, Zhang.et al*. "Development and testing of a motor drive and control unit based on the field-oriented control algorithm for the seed-metering device", Computers and Electronics in Agriculture, **vol. 211**, no.108024, 2023, pp. 1-13. Beijing: Elsevier B.V.

[3] *YF, Yao. XG, Chen. C, Ji.et al*. "Design and experiments of the single driver for maize precision seeders based on fuzzy PID control", Transactions of the Chinese Society of Agricultural Engineering, **vol. 38**, no.6, 2022, pp. 12-21. Beijing: CSAE.

[4] *YQ, Ding. XT, He. L, Yang.et al*. "Low-cost turn compensation control system for conserving seeds and increasing yields from maize precision planters", Computers and Electronics in Agriculture, **vol. 199**, no.107118, 2022, pp. 1-13. Beijing: Elsevier B.V.

[5] *S, Wang. Y, Sun. C, Yang.et al*. "Advanced design and tests of a new electrical control seeding system with genetic algorithm fuzzy control strategy", Journal of Computational Methods in Sciences and Engineering, **vol. 21**, no.3, 2021, pp. 703-712. IOS Press BV.

[6] *CK, Wen. J, Zhang. K, Zheng. et al*. "Accelerated verification method for the reliability of the motor drive mechanism of the corn precision seed-metering device", Computers and Electronics in Agriculture, **vol. 212**, no.108163, 2023, pp. 1-23. Beijing: Elsevier B.V.

[7] *XY, Yan. JP, Hu. J, Ma.et al*. "Design of a control system for magnetic plate-type precision seeding production line based on PLC and MCU", Open Electrical and Electronic Engineering Journal, **vol. 8**, no.1, 2013, pp. 1-7. Bussum: Bentham Science Publishers B.V.

[8] *SH. Ren, SJ. Yi*. "Control Mechanism and Experimental Study on Electric Drive Seed Metering Device of Air Suction Seeder", Tehnicki Vjesnik, **vol. 29**, no.4, 2022, pp.1254– 1261. Strojarski Facultet.

[9] *J. Chen, YQ. Yan, XD. Zhang et al*. "DESIGN OF CONTROL SYSTEM OF SEED METERING DEVICE TEST - BED BASED ON FUZZY PID", INMATEH - Agricultural Engineering, **vol. 67**, no.2, 2022, pp.509 - 524. INMA Bucharest.

[10] *LQ. Chen, GK. Lv, CM. Cao*. "Development and evaluation of motor - driven greenhouse mini - seeder using modal analysis", International Agricultural Engineering Journal, **vol. 22**, no.3, 2013, pp.95 - 103.

[11] *XY. Yan, JP. Hu, J. Ma, X. Wang*. "Design of a control system for magnetic plate - type precision seeding production line based on PLC and MCU", Open Electrical and Electronic Engineering Journal, **vol. 8**, no.1, 2013. Bentham Science Publishers B.V., P.O. Box 294, Bussum, 1400 AG, Netherlands.

[12] *P. Gautam, H. Kushwaha, A. Kumar et al*. "Microcontroller - based Low - cost Seed Metering Module Retrofit on Cultivator", Indian Journal of Engineering and Materials Sciences, **vol. 30**, no.1, 2023, pp.180 - 188.

[13] *R. Strasser, S. Badua, A. Sharda et al*. "Performance of planter electric - drive seed meter during simulated planting scenarios", Applied Engineering in Agriculture, **vol. 35**, no.6, 2019, pp.925 - 935.

[14] *X. Jin, J. Liu, Z. Chen et al*. "Precision control system of rice potting and transplanting machine based on GA - Fuzzy PID controller", Computers and Electronics in Agriculture, **vol. 220**, 2024, pp. Elsevier B.V.